



# Multivalent protein binding in carbohydrate-functionalized monolayers through protein-directed rearrangement and reorientation of glycolipids at the air–water interface

Haifu Zheng, Xuezhong Du\*

Key Laboratory of Mesoscopic Chemistry (Ministry of Education), State Key Laboratory of Coordination Chemistry, and School of Chemistry and Chemical Engineering, Nanjing University, Nanjing 210093, People's Republic of China

## ARTICLE INFO

### Article history:

Received 6 December 2010

Received in revised form 5 April 2011

Accepted 7 April 2011

Available online 25 May 2011

### Keywords:

Infrared spectroscopy

Surface plasmon resonance

Aqueous monolayer

Lipid rearrangement

Multivalent protein binding

## ABSTRACT

Multivalent protein binding plays an important role not only in biological recognition but also in biosensor preparation. Infrared reflection absorption spectroscopy and surface plasmon resonance techniques have been used to investigate concanavalin A (Con A) binding to binary monolayers composed of 1,2-di-*O*-hexadecyl-*sn*-glycerol and derived glycolipids with the mannose moieties. The glycolipids in the binary monolayers at the air–water interface underwent both lateral rearrangement and molecular reorientation directed by Con A in the subphase favorable to access of the carbohydrate ligands to protein binding pockets for the formation of multivalent binding sites and the minimization of steric crowding of neighboring ligands for enhanced binding. The amounts of specifically bound proteins in the binary monolayers at the air–water interface were accordingly increased in comparison with those in the initially immobilized monolayers at the air–water interface. The directed rearranged binary monolayers with multivalent protein binding were preserved for the preparation of biosensors.

© 2011 Elsevier B.V. All rights reserved.

## 1. Introduction

Protein–carbohydrate interactions play a key role in many cellular processes including cell differentiation, fertilization [1], adhesion, inflammation [2], cell–cell communication [3], and immune response [4]. These specific binding events happen through glycoproteins, glycolipids, and polysaccharides on cell surfaces and carbohydrate-binding lectins.<sup>1</sup> Lectins typically possess shallow binding pockets exposure to solvents, thus the monovalent protein–carbohydrate interactions are generally weak [5,6]. It is possible for the lectins to participate in multivalent binding or several simultaneous binding events for improved interaction strength and specificity [5]. Multivalent protein binding may achieve higher binding affinity, allow signaling through oligomerization, and induce changes in the distribution of molecules at the membrane surface [7,8]. On the other hand, multivalent interactions are crucial for discovering a broad range of biosensors for use in medicine, environment, and food processing [8]. The intricacy of the cell membrane structures along with the highly dynamic nature of lipid–lipid and lipid–protein interactions in the cell membranes make the biophysical interactions very difficult to investigate and understand in real time [9]. Langmuir monolayers have half a structure of cell membranes and offer a simple system to

mimic cell surface rearrangement due to the lateral mobility of the lipid components at the air–water interface [9–12]. Lipid components can rearrange to form well-matched interactions with proteins through multivalent binding. The organized monolayers of glycolipids containing mono-saccharide moieties at the air–water interface might act as multiple carbohydrate ligands along polymer backbones due to the hydrophobic interactions between the corresponding alkyl chains, moreover the spatial distribution of the carbohydrate ligands can be adjusted due to lateral rearrangement of the glycolipids.

Concanavalin A (Con A, pI 4.5–5.6) [13] is a multivalent binding protein and exists as a tetramer (104 kDa) at pH > 7.0. Con A can be capable of specifically binding mannose moieties in the presence of Mn<sup>2+</sup> and Ca<sup>2+</sup> ions [14,15]. The Con A tetramer has four carbohydrate-binding sites and presents two binding sites on each face [16]. Self-assembled monolayers (SAMs) [17–21], vesicles [7,22,23], and supported lipid bilayers (SLBs) [24,25] have been also used for model systems to study the protein–carbohydrate interactions. It has been shown that the surface density and spatial arrangement of the carbohydrate ligands play a crucial role in protein binding [5,17,21]. On one hand, the surface ligand densities in the three types of model systems cannot be accurately controlled because they are formed from bulk solutions in comparison with Langmuir monolayers at the interface, and the covalent immobilization of lipids in SAMs obviously suppresses ligand spatial distribution and multivalent protein binding. On the other hand, the influence of spatial arrangement of carbohydrate ligands on the protein binding is still largely unclear.

\* Corresponding author. Fax: +86 25 83317761.

E-mail address: [xzdu@nju.edu.cn](mailto:xzdu@nju.edu.cn) (X. Du).

The surface densities of different components in Langmuir monolayers can be accurately controlled, and the lipid components are capable of lateral mobility. The favorable spatial arrangement of the glycolipids in Langmuir monolayers through lateral mobility could facilitate enhancement of multivalent protein binding.

Con A binding to the binary monolayers composed of double-chained glycolipids and protein-repelling lipids with oligo(ethylene glycol) (OEG) spacers/moieties, [8-(1,2-di-*O*-hexadecyl-*sn*-glycer-3-oxy)-3,6-dioxaoctyl]- $\alpha$ -*D*-mannopyranoside (DPEM) and 1,2-di-*O*-hexadecyl-3-*O*-[8-hydroxy-3,6-dioxaoctyl]-*sn*-glycerol (DPE), has been recently studied in detail [26,27]. The OEG moieties are known to well resist nonspecific protein binding, in addition, the flexible OEG spacers/moieties were favorable to access of carbohydrate ligands to protein binding pockets to form multivalent interactions, even in the absence of lack of glycolipid rearrangement and reorientation. This paper is to investigate Con A binding to the binary monolayers consisting of glycolipids and lipids without OEG spacers/moieties, (1,2-di-*O*-hexadecyl-*sn*-glycer-3-oxy)- $\alpha$ -*D*-mannopyranoside (DPM) and 1,2-di-*O*-hexadecyl-*sn*-glycerol (DPG) (Fig. 1) for deeper understanding of the relationship between multivalent protein binding and glycolipid rearrangement/reorientation. In general, the hydroxyl (OH) groups are not good protein-resistant moieties, but the DPG monolayer displayed excellent properties of resisting nonspecific Con A binding. The glycolipids without OEG spacers in the binary monolayers underwent a change in hydrocarbon chain orientation in the presence of Con A as well as spatial rearrangement of the carbohydrate ligands for multivalent protein binding. The reorientation of DPM and DPG in the binary monolayers compensated for local adjustment of OEG spacers/moieties of DPEM and DPE.

## 2. Materials and methods

### 2.1. Materials

DPM and DPG were synthesized according to the methods reported recently [26,28], and their chemical structures were confirmed by NMR spectra (500 MHz, Bruker DRX-500). They were solubilized in pretreated chloroform (analytical grade) to be a concentration of 1 mM and stored at  $-20^{\circ}\text{C}$  prior to use. Their binary mixtures were prepared volumetrically from respective stock solutions. 1-Octadecanethiol (ODT, 95%) was purchased from Fluka. Triton X-100, ethanol, NaCl, and NaOH were of analytical grade. Con A from

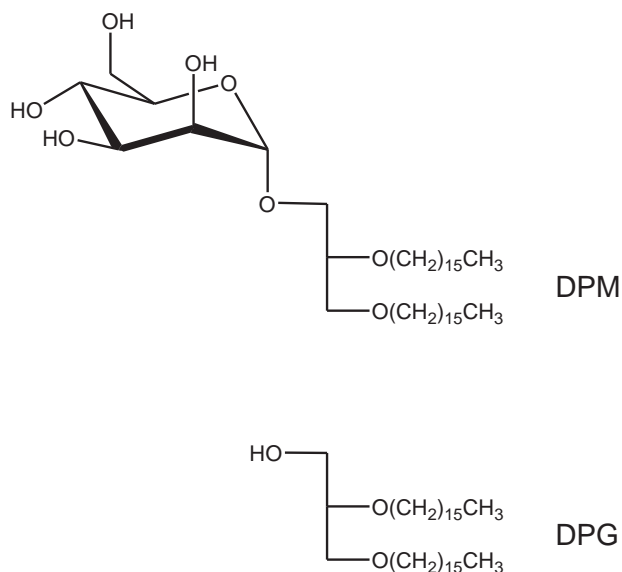


Fig. 1. Chemical structures of DPM and DPG.

*Canavalia ensiformis* (Type V) was purchased from Sigma. Water used was double-distilled (pH 5.6, resistivity 18.2 M $\Omega$  cm, surface tension 73.06 mN/m at 22  $^{\circ}\text{C}$ ) after a deionized exchange. The aqueous solutions of Con A and subphases were prepared from phosphate buffered saline (PBS, 10 mM phosphate, 0.1 mM Mn $^{2+}$ , 0.1 mM Ca $^{2+}$ , and 150 mM NaCl, pH 7.4).

### 2.2. Infrared reflection absorption spectroscopy (IRRAS) measurements

In situ IRRAS spectra of the monolayers at the air–water interface were recorded on an Equinox 55 FTIR spectrometer connected to an XA-511 external reflection attachment with a shuttle trough system and a narrow band mercury-cadmium-telluride (MCT) detector (Bruker Optics) [27,29]. IRRAS data are defined as plots of reflectance-absorbance (RA) versus wavenumber,  $RA = -\log(R/R_0)$ , where  $R$  and  $R_0$  are the reflectivities of the film-covered and film-free surfaces, respectively. The sample (30 cm  $\times$  7 cm  $\times$  0.5 cm) and reference (8 cm  $\times$  7 cm  $\times$  0.5 cm) troughs were fixed on a shuttle device driven by a computer-controlled stepper motor for allowing spectral collections from the two troughs in an alternating fashion. A KRS-5 polarizer was used to generate p- and s-polarized beams. The film constituents were spread from their chloroform solutions onto the sample trough, and 20 min was allowed for solvent evaporation. The attachment system was then enclosed for humidity equilibrium for 4 h, and then the monolayers were discontinuously compressed to the desired surface pressure of 30 mN/m from  $\sim$ 0 mN/m. After 30 min of relaxation, the two moving barriers were stopped and the areas of the monolayers were kept constant. Upon protein binding, concentrated Con A solutions were injected into the unstirred subphase beneath the compressed monolayers at 30 mN/m behind the barriers with an L-shaped syringe. The external reflection absorption spectra of the PBS solutions containing Ca $^{2+}$  and Mn $^{2+}$  were used as a reference. These spectra were recorded with a resolution of 8 cm $^{-1}$  by coaddition of 1024 scans at 22  $^{\circ}\text{C}$ .

### 2.3. Surface plasmon resonance (SPR) measurements

SPR technique can optically monitor changes of refractive index in the vicinity of sensor surfaces in real time without analyte labeling [20,30,31]. The technique was employed to investigate protein binding processes at the solid–water interface and the data came from the direct binding of soluble proteins in aqueous solutions. Integrated optics SPR sensors (Spreeta, Texas Instruments) were used to measure protein binding kinetics for the monolayers [11,12]. The Spreeta sensors combined the sensor surfaces with all optic and electronic components required for SPR experiments in a compact and lightweight assembly [30,31]. A Teflon microtrough was homemade with the dimensions of 4 cm  $\times$  2 cm  $\times$  1 cm [29,32]. The trough walls were undercut by 45 $^{\circ}$  to eliminate the formation of a meniscus presenting a planar interface [33]. The SPR sensor was first cleaned with an aqueous solution of 1% Triton X-100 and 0.1 M NaOH followed by copious double-distilled water. The sensor surface was modified to be hydrophobic by immersion in an ODT solution in absolute ethanol (2 mM) for 20 min followed by rinsing with copious double-distilled water. A binary monolayer was spread until the desired surface pressure 30 mN/m was reached, and then it was allowed for relaxation for 1 h. The ODT-modified SPR sensor was horizontally lowered into contact with the monolayer and brought to a depth of about 1–2 mm. This procedure was equivalent to a horizontal monolayer transfer to a solid substrate but without ever removing the substrate coated with the transferred monolayer from the trough. After a period of 10 min to ensure the integrity of the transferred monolayer, the protein solution of desired volume was injected into the subphase to reach a final Con A concentration of 100  $\mu\text{g}/\text{mL}$ . The protein binding was allowed to proceed for 1.5 h for the binary monolayers. The sensor surface was then flushed with PBS solutions

for the removal of nonspecifically bound Con A, the subphase was then exchanged with acetate buffer (pH 1.5) to remove specifically bound proteins for regeneration and finally with PBS solution prior to reintroducing Con A for subsequent binding.

In the case of the monolayers at the air–water interface, Con A was first injected beneath the monolayer after 1 h of relaxation and allowed for protein binding to the binary monolayers for 1.5 h. SPR signals were recorded until an ODT-modified SPR sensor was brought into contact with the protein-bound monolayer. The following procedures were the same as those in the case of the initially immobilized monolayers.

### 3. Results and discussion

#### 3.1. Molecular assemblies of binary monolayers at the air–water interface

The IRRAS spectra of the monolayers of DPM, DPG, and their binary mixtures with different mole fraction of DPM ( $X_{\text{DPM}}$ ) at the air–water interface are shown in Fig. 2. These spectral baselines in the region  $1750\text{--}1600\text{ cm}^{-1}$  were distorted as positive bands because of the altered structure of the water adjacent to the headgroups of the film constituents, however, these monolayers displayed similar spectral behaviors. At the low surface pressure of  $5\text{ mN/m}$ , two strong bands

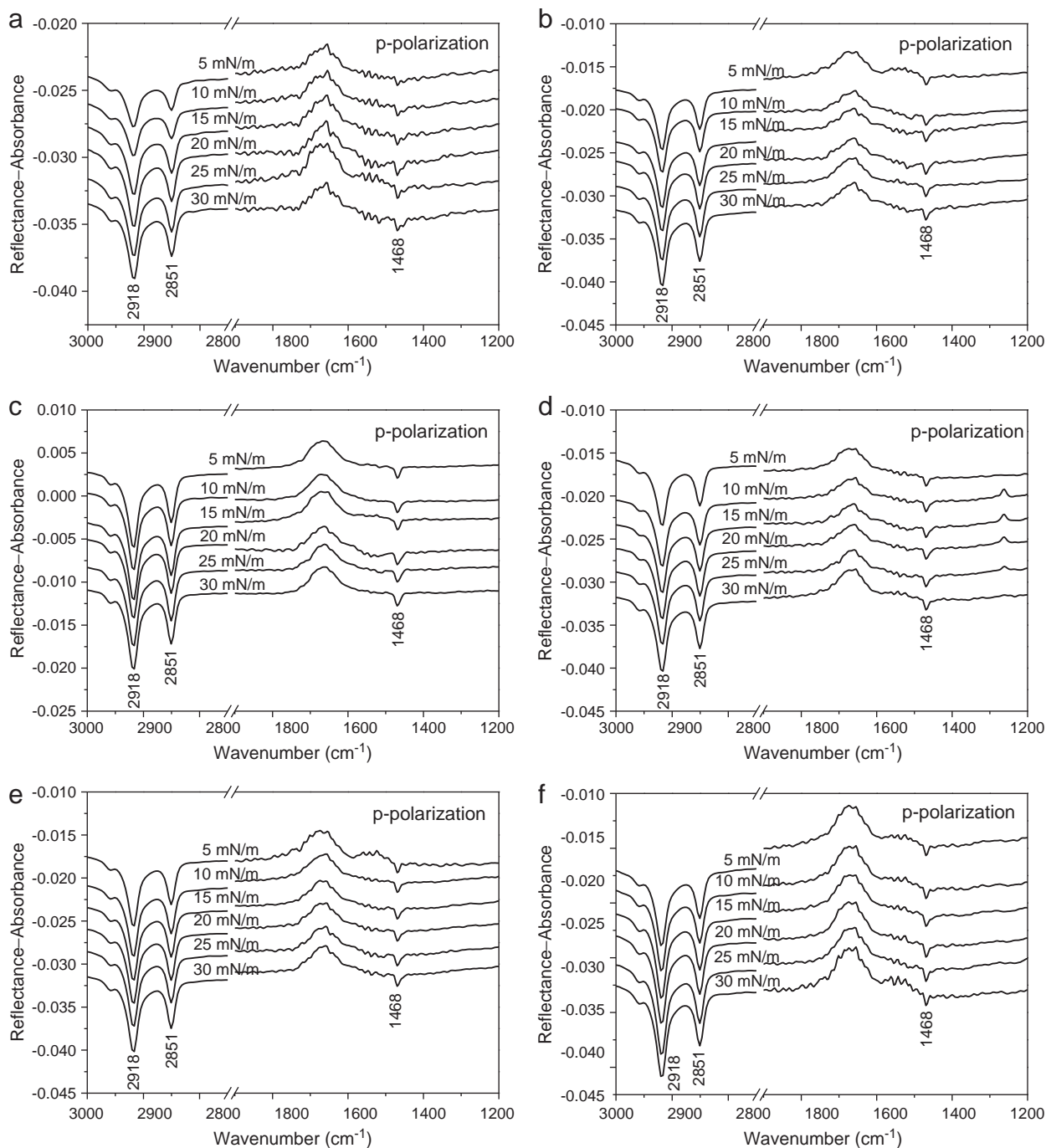


**Fig. 2.** p-Polarized IRRAS spectra of the monolayers of DPM, DPG, and their binary mixtures on the PBS solution (pH 7.4) containing  $\text{Ca}^{2+}$  and  $\text{Mn}^{2+}$  at various surface pressures at an incidence angle of  $30^\circ$  at  $22^\circ\text{C}$ : (a) DPG; (b)  $X_{\text{DPM}} = 0.1$ ; (c)  $X_{\text{DPM}} = 0.2$ ; (d)  $X_{\text{DPM}} = 0.3$ ; (e)  $X_{\text{DPM}} = 0.4$ ; (f) DPM.

appeared at 2918 and 2851  $\text{cm}^{-1}$ , assigned to the antisymmetric and symmetric  $\text{CH}_2$  stretching vibrations [ $\nu_a(\text{CH}_2)$  and  $\nu_s(\text{CH}_2)$ ] of alkyl chains, respectively. Upon gradual increase of surface pressure to 30 mN/m, a slight increase in band intensity was observed, but the band frequencies remained unchanged. It is well-known that the  $\nu_a(\text{CH}_2)$  and  $\nu_s(\text{CH}_2)$  frequencies are sensitive to conformation order of alkyl chains, particularly for the  $\nu_a(\text{CH}_2)$  modes. Lower wavenumbers around 2916–2918 and 2848–2850  $\text{cm}^{-1}$  are characteristic of highly ordered chains in *all-trans* conformations, while higher wavenumbers around 2924–2926 and 2854–2856  $\text{cm}^{-1}$  are indicative of highly disordered chains with significant *gauche* conformations [34]. It is clear that the alkyl chains in these monolayers were highly ordered with fewer *gauche* defects irrespective of surface pressure. The spectral behaviors of the monolayers of DPM, DPG, and their binary mixtures were different from those of their counterparts with OEG spacers/moieties. The alkyl chains in the monolayers of DPEM, DPE, and their binary mixtures underwent a change from highly disordered structures to highly ordered ones with the increase of surface pressure, intimately associated with the mushroom-like to brush conformation transition of the OEG spacers/moieties [27]. At the surface pressures investigated here, a weak band at 1468  $\text{cm}^{-1}$  was observed for these monolayers, attributed to the  $\text{CH}_2$  scissoring vibration [ $\delta(\text{CH}_2)$ ]. The appearance of the singlet peak at 1468  $\text{cm}^{-1}$  indicated that the alkyl chains in the monolayers were probably packed in a hexagonal subcell structure where each chain could freely rotate around its axis [35].

### 3.2. Protein-directed rearrangement of glycolipids at the air–water interface

It is shown that the monolayers at 30 mN/m were enough to inhibit proteins from penetrating into the hydrophobic regions besides being capable of lateral mobility [36]. The surface pressure of 30 mN/m is equivalent to the lateral pressures estimated for cell membranes under physiological conditions [37,38]. The IRRAS spectra of injection of Con A beneath the individual monolayer of DPG at the air–water interface at 30 mN/m are shown in Fig. 3. The spectrum after 10 h was factually identical to that prior to protein injection, which indicates that Con A could not be adsorbed onto the DPG monolayer in this case. Obviously, the DPG monolayer displayed excellent properties of resisting nonspecific Con A binding although the OH groups are not good protein-repelling moieties. Even at 5 and 15 mN/m, no Con A binding to the DPG monolayers was observed because the DPG lipids without flexible OEG moieties formed liquid-condensed monolayers at various pressures to prevent protein binding (Fig. S1 in Appendix A).

Con A binding to the binary monolayers of DPM and DPG with different  $X_{\text{DPM}}$  was clearly observed (Fig. 3). The injection of proteins resulted in the appearance of amide I and amide II bands around 1640 and 1535  $\text{cm}^{-1}$ , respectively. The two bands are more evident from their difference spectra after and before protein binding. In contrast to the protein-repelling DPG monolayer, the observed amide I and amide II bands reflected specific protein binding to the binary monolayers. Amide I bands are contributed primarily from the C=O stretching vibration of the peptide bonds, and amide II bands are due to the mixed modes of C–N stretching and N–H bending vibrations. There are well-established empirical correlations between amide I band frequencies and protein secondary structures [39–41]. Second derivatives of their difference spectra in the region 1700–1600  $\text{cm}^{-1}$  at protein binding saturation are shown in Fig. S2. The amide I bands consisting of a significant amount of the component around 1640  $\text{cm}^{-1}$  and a small amount of the component around 1680  $\text{cm}^{-1}$ . It is known that both a strong band  $\leq 1640 \text{ cm}^{-1}$  (1630–1640  $\text{cm}^{-1}$ ) and a weak band  $\geq 1680 \text{ cm}^{-1}$  are characteristic of  $\beta$ -sheet structures [42,43]. It is obvious that the specifically bound Con A possessed a great amount of antiparallel  $\beta$ -sheet conformations, which is in good agreement with

the secondary structures of native Con A composed of predominant  $\beta$ -sheet conformations without  $\alpha$ -helix one [14,42,43]. The spectral features indicate that the secondary structures of the proteins almost remained unchanged upon binding to the hydrophilic moieties of the binary monolayers.

Seen from the difference spectra after and before protein binding with different  $X_{\text{DPM}}$  to the same scale (Fig. 3), the intensities of the amide I bands at  $X_{\text{DPM}} = 0.1$  and 0.2 were stronger than those at  $X_{\text{DPM}} = 0.3$  and 0.4. This is different from the Con A binding behaviors for the binary monolayers of DPEM and DPE at the air–water interface with comparable amide I band intensities independent of  $X_{\text{DPEM}}$  [27]. It has been shown that the surface density and spatial arrangement of the carbohydrate ligands play a crucial role in Con A binding [5,17,21,26] and that the amount of specifically bound proteins was finally determined by the balance between them [26]. Low surface ligand densities would limit multivalent protein binding considering the separation distance of about 6.5 nm between two binding pockets of Con A [44], while high surface densities might result in steric crowding of neighboring ligands, which inhibits access of the ligands to protein binding pockets. It is obvious that favorable spatial arrangement of the glycolipids can alleviate the steric crowding of neighboring ligands and facilitate the multivalent protein binding even at a specific surface ligand density. The glycolipids in the binary monolayers at the air–water interface underwent a lateral reorganization to develop a new spatial arrangement directed by Con A in the subphase. The optimal spatial arrangement of the ligands at the interface could match well with the protein binding pockets and simultaneously minimize the steric crowding of neighboring ligands. The spatial rearrangement of the glycolipids at the air–water interface promoted the formation of a great number of multivalent binding sites to meet the separation distance between the protein binding pockets, so that the amounts of specifically bound proteins were accordingly increased. At  $X_{\text{DPM}} = 0.3$  and 0.4, the steric crowding of neighboring ligands could not be significantly reduced through the lateral rearrangement of DPM, so that the amounts of specifically bound Con A were not so high as those at low  $X_{\text{DPM}}$ . It is most likely that the lack of flexible OEG spacers/moieties was an unfavorable factor for ready access of the ligands to the protein binding pockets at high  $X_{\text{DPM}}$ .

Before and after protein binding, the  $\nu_a(\text{CH}_2)$  and  $\nu_s(\text{CH}_2)$  frequencies of the alkyl chains in the binary monolayers almost remained constant. Seen from their difference spectra, the presence of two weak positive peaks at 2918 and 2851  $\text{cm}^{-1}$  at various  $X_{\text{DPM}}$  indicates that the alkyl chains were tilted to a certain degree after protein binding. Furthermore, the orientation angles of the alkyl chains in the binary monolayers before and after protein binding were quantitatively determined by the fit of theoretical calculations to the experimental data of the  $\nu_a(\text{CH}_2)$  bands [45–48] (Figs. S3–S6) and listed in Table 1. The tilt angle of the alkyl chains were 10–20° with respect to the normal of the monolayers before protein binding and were increased to 15–25° after protein binding dependent on  $X_{\text{DPM}}$ . For the binary monolayers of DPEM and DPE at the air–water interface, the alkyl chains remained unchanged before and after Con A binding except for  $X_{\text{DPEM}} = 0.2$  [27]. The lack of flexible OEG spacers/moieties led to the reorientation of the glycolipids to match with the protein binding pockets instead of local adjustment through the OEG spacers as for the binary monolayers of DPEM and DPE. Yim et al. investigated myoglobin/lysozyme binding to the Langmuir monolayers of metal ion chelating lipids 1,2-distearyl-*rac*-glycero-3-triethyleneoxide iminodiacetic acid (DSIDA) at 35–40 mN/m using grazing incidence X-ray reflection (GIXD) technique and found an increase in the size of hexagonal unit cell and tilt angle of the alkyl chains in the presence of proteins due to lipid rearrangement and multiple site binding [49]. It is clear that the protein-directed rearrangement of the glycolipids in the monolayers not only matched with the protein binding pockets and reduced the steric crowding of

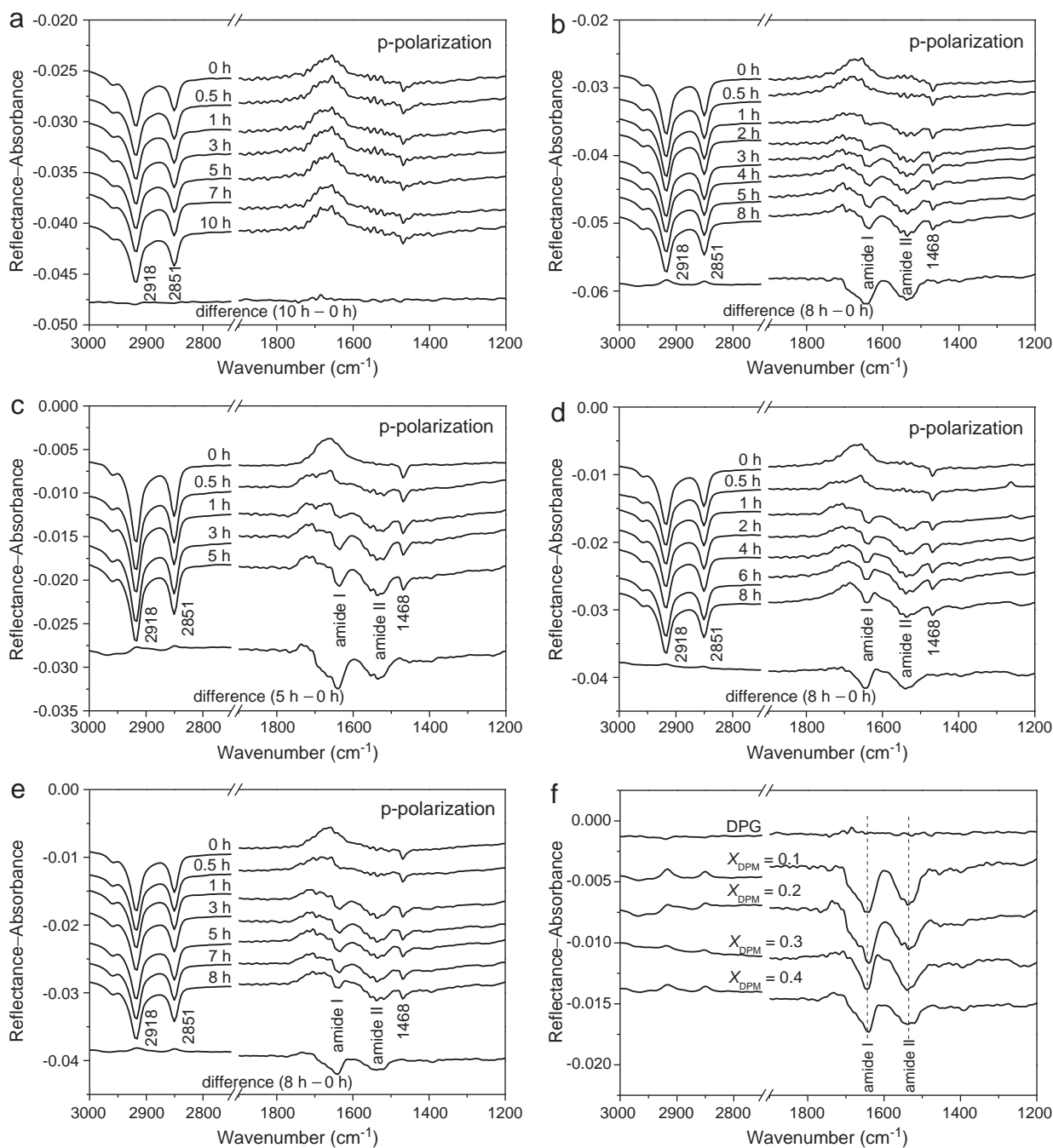


**Fig. 3.** Time-dependent p-polarized IRRAS spectra of the individual monolayer of DPG and binary monolayers of DPM and DPG on the PBS solution (pH 7.4) containing  $\text{Ca}^{2+}$  and  $\text{Mn}^{2+}$  at the surface pressure 30 mN/m at an incidence angle of  $30^\circ$  at  $22^\circ\text{C}$  upon Con A binding: (a) DPG; (b)  $X_{\text{DPM}} = 0.1$ ; (c)  $X_{\text{DPM}} = 0.2$ ; (d)  $X_{\text{DPM}} = 0.3$ ; (e)  $X_{\text{DPM}} = 0.4$ ; (f) difference spectra after and before protein binding.

neighboring ligands but also adjusted molecular orientations for the development of multivalent protein binding.

### 3.3. Multivalent protein binding in the binary monolayers

In order to monitor protein binding to the binary monolayers using the SPR technique, the hydrophobically modified sensor surfaces have to contact the monolayers at the air–water interface tightly. If the monolayers were first horizontally immobilized with the sensors followed by protein injection beneath the monolayers, such monolayers are referred to as control ones. For the individual monolayer of DPG, negligible specific Con A binding was observed (Fig. S7), and for

the control binary monolayers of DPM and DPG (Fig. 4), significant specific Con A binding was detected. The amounts of specifically bound proteins during the initial binding stages (estimated on the basis of an SPR angle shift of  $0.1^\circ$ –a protein surface density of  $0.1 \mu\text{g}/\text{cm}^2$ ) [50] as a function of  $X_{\text{DPM}}$  are shown in Fig. 5. The amount was high at  $X_{\text{DPM}} = 0.1$  followed by a drop at  $X_{\text{DPM}} = 0.2$ , then increased gradually upon further increase of  $X_{\text{DPM}}$ . A similar case was observed for the control binary monolayers of DPEM and DPE [26]. The amount of specifically bound Con A was related not only to surface density of the ligands but also to steric crowding of neighboring ligands and ultimately determined by the balance between them. In the control binary monolayers, the spatial arrangement of the

**Table 1**

Orientation angles of the hydrocarbon chains in the binary monolayers before and after Con A binding.<sup>a</sup>

Monolayer	Subphase	Tilt angle (°)
$X_{\text{DPM}} = 0.1$	Water	10
	Con A	25
$X_{\text{DPM}} = 0.2$	Water	10
	Con A	15
$X_{\text{DPM}} = 0.3$	Water	20
	Con A	25
$X_{\text{DPM}} = 0.4$	Water	20
	Con A	25

<sup>a</sup>  $\theta$ , orientation angle of chain axis;  $k_{\text{max}} = 0.80$ , maximum extinction coefficient;  $\alpha = 90^\circ$ , angle between  $\nu_{\text{a}}(\text{CH}_2)$  vibrational dipole moment and chain axis;  $L = 2.05$  nm, extended chain length;  $n_{\text{ord}} = 1.46$  and  $n_{\text{ext}} = 1.57$ , ordinary and extraordinary refractive indexes;  $\Gamma = 98.7\%$ , polarizer efficiency.

two lipid components was only determined by the interactions between them. The change of the amounts of specifically bound proteins with  $X_{\text{DPM}}$  (SPR results) was different from that for the binary monolayers at the air–water interface (IRRAS results), where the protein-directed rearrangement of glycolipids was developed. In order to verify the formation of the new spatial arrangement of the ligands, the SPR technique was further applied to investigate protein binding to the rearranged binary monolayers (Fig. 4). For the initial protein binding to the binary monolayers at the air–water interface, the binding kinetics were not attained because the SPR sensors could not be in contact with the monolayers if they were to remain laterally mobile. However, the final adsorption amounts could be obtained by horizontally placing the hydrophobically modified SPR sensors

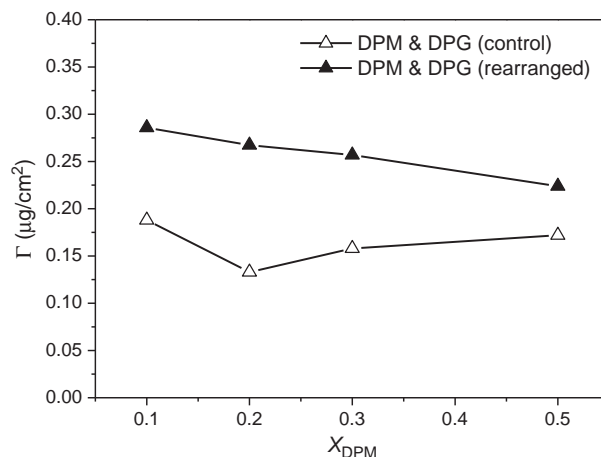


**Fig. 5.** Amounts of specifically bound Con A on the rearranged and control monolayers of DPM and DPG at saturation as a function of surface density of glycolipids.

in contact with the monolayers after identical binding times. The fabrication of the rearranged monolayers was simply a two-dimensional version (protein surface imprinting) of the solution-phase interactions between templates and functional monomers for the preparation of molecularly imprinted materials [51,52]. At a specific  $X_{\text{DPM}}$ , the initially fluid and control monolayers had the same surface densities because the identical amounts of the lipid components were spread at the fixed trough area to reach the desired surface

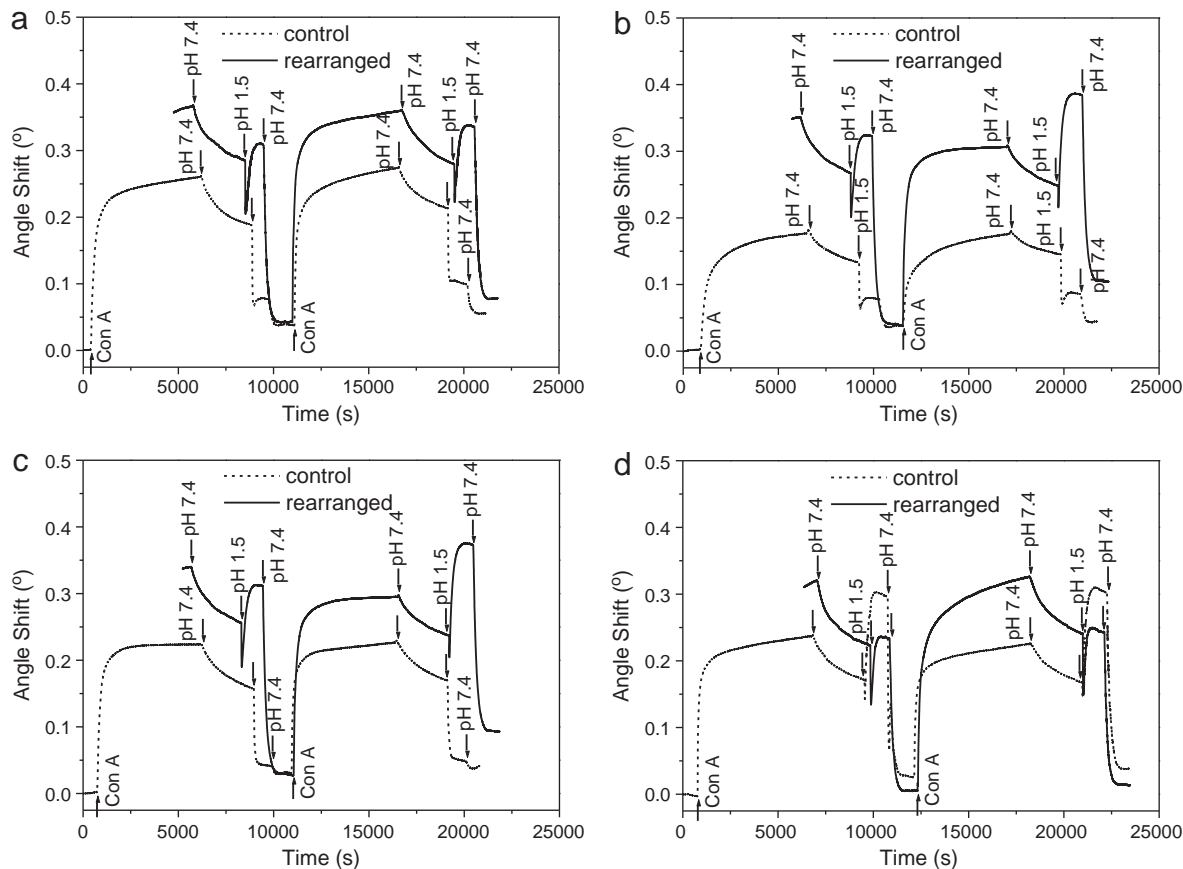


**Fig. 4.** SPR sensorgrams of Con A binding to and unbinding from the surfaces of rearranged and control binary monolayers of DPM and DPG at the surface pressure 30 mN/m with different  $X_{\text{DPM}}$  upon injection of Con A with a final concentration of 100  $\mu\text{g}/\text{mL}$  followed by rinsing respectively with PBS solution (pH 7.4) and acetate buffer (pH 1.5): (a)  $X_{\text{DPM}} = 0.1$ ; (b)  $X_{\text{DPM}} = 0.2$ ; (c)  $X_{\text{DPM}} = 0.3$ ; (d)  $X_{\text{DPM}} = 0.5$ .

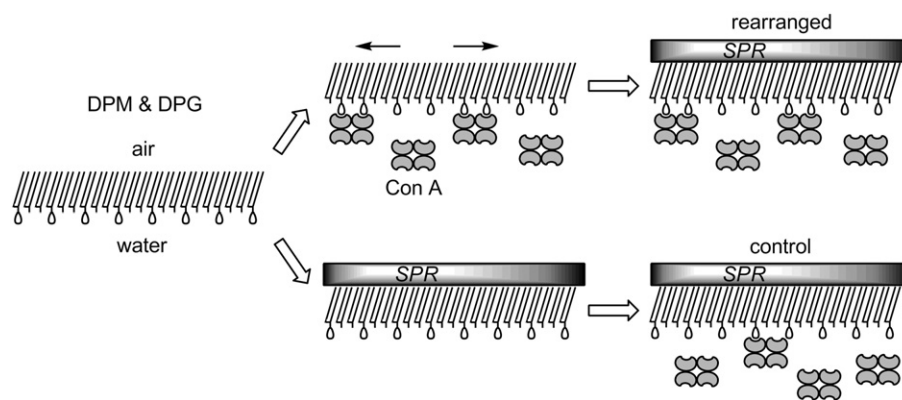


**Fig. 6.** Schematic illustration of Con A binding to rearranged and control binary monolayers of DPM and DPG.

pressures. Interestingly, the amounts of specifically bound proteins on the rearranged monolayers were increased in comparison with those on the control monolayers. There was significant improvement in protein binding at  $X_{\text{DPM}} = 0.2$  in contrast to the most inhibited protein binding for the corresponding control monolayers. The favorable spatial arrangement of the ligands in the rearranged monolayer facilitated to create multivalent binding sites for the proteins and the steric crowding of neighboring ligands was substantially reduced. At  $X_{\text{DPM}} = 0.1$ , the amount of specifically bound proteins on the rearranged one was further increased although the amount was high for the control monolayer. At  $X_{\text{DPM}} = 0.5$ , the amount on the rearranged monolayer was slightly improved. This was because the lateral reorganization of the glycolipids could not cause a significant change in spatial arrangement of the ligands due to the excess glycolipids. It was difficult to reduce substantially the steric crowding of neighboring ligands at high surface ligand densities. The increase of the surface ligand densities could simultaneously increase the probabilities of multivalent protein binding and steric ligand crowding in the control monolayers. The spatial rearrangement of the ligands in the rearranged monolayers facilitated the formation of multivalent binding sites at various surface densities, but the steric crowding of neighboring ligands gradually became evident with the increase of surface densities although its influence was not so significant as in the control monolayers.

These changes in protein binding indicate that there were different spatial arrangements of the ligands between the rearranged and control monolayers. The illustrations of Con A binding to the rearranged and control binary monolayers are schematically presented in Fig. 6. The Con A-directed assembly of the binary monolayers at the air–water interface gave rise to a new spatial arrangement of the ligands to match well with the protein binding pockets for multivalent protein binding and to enhance protein binding.

Both the rearranged and control monolayers of DPM and DPG could be nearly regenerated after the specifically bound proteins were washed with acetate buffer (pH 1.5) followed by the initial PBS buffer (Fig. 4). The amounts of specifically bound proteins at saturation and/or protein binding kinetics during the rebinding stages were almost the same as those during the initial binding stages. It means that the favorable spatial arrangement of the ligands in the monolayers at the air–water interface well suited for the multivalent protein binding was preserved for the subsequent binding events in the preparation of biosensors.

#### 4. Conclusion

The alkyl chains in the monolayers of DPM, DPG, and their binary mixtures at the air–water interface were almost highly ordered independent of surface pressure. The amounts of specifically bound proteins in the binary monolayers at the air–water interface were

increased in comparison with those in the initially immobilized monolayers, where the binding amount was high at  $X_{\text{DPM}} = 0.1$  followed by a drop at  $X_{\text{DPM}} = 0.2$ , and then increased gradually upon further increase of  $X_{\text{DPM}}$ . The amount of specifically bound proteins is closely related to surface density and spatial arrangement of the carbohydrate ligands. The glycolipids in the binary monolayers at the air–water interface underwent lateral rearrangement and molecular reorientation directed by Con A in the subphase favorable to access of the ligands to protein binding pockets for the formation of multivalent binding sites and the minimization of steric crowding of neighboring ligands for enhanced binding. The directed rearranged binary monolayers with multivalent protein binding were preserved for the preparation of biosensors.

#### Acknowledgements

This work was supported by the National Natural Science Foundation of China (Grants 20673051 and 20873062) and the program for New Century Excellent Talents in University (NCET-07-0412).

#### Appendix A. Supplementary data

Supplementary data to this article can be found online at [doi:10.1016/j.bbame.2011.04.019](https://doi.org/10.1016/j.bbame.2011.04.019).

#### References

- [1] N. Sharon, H. Lis, Lectins as cell recognition molecules, *Science* 246 (1989) 227–234.
- [2] C.R. Bertozzi, L.L. Kiessling, Chemical glycobiology, *Science* 291 (2001) 2357–2364.
- [3] K.T. Pilobello, L.K. Mahal, Deciphering the glycode: the complexity and analytical challenge of glycomics, *Curr. Opin. Chem. Biol.* 11 (2007) 300–305.
- [4] L.L. Kiessling, J.E. Gestwicki, L.E. Strong, Synthetic multivalent ligands in the exploration of cell–surface interactions, *Curr. Opin. Chem. Biol.* 4 (2000) 696–703.
- [5] E.A. Smith, W.D. Thomas, L.L. Kiessling, R.M. Corn, Surface plasmon resonance imaging studies of protein–carbohydrate interactions, *J. Am. Chem. Soc.* 125 (2003) 6140–6148.
- [6] P.-H. Liang, S.-K. Wang, C.-H. Wong, Quantitative analysis of carbohydrate–protein interactions using glycan microarrays: determination of surface and solution dissociation constants, *J. Am. Chem. Soc.* 129 (2007) 11177–11184.
- [7] G.B. Thomas, L.H. Rader, J. Park, L. Abezgauz, D. Danino, P. DeShong, D.S. English, Carbohydrate modified cationic vesicles: probing multivalent binding at the bilayer interface, *J. Am. Chem. Soc.* 131 (2009) 5471–5477.
- [8] T. Yang, O.K. Baryshnikova, H. Mao, M.A. Hojden, P.S. Cremer, Investigations of bivalent antibody binding on fluid-supported phospholipid membranes: the effect of hapten density, *J. Am. Chem. Soc.* 125 (2003) 4779–4784.
- [9] C. Peetla, A. Stine, V. Labhasetwar, Biophysical interactions with model lipid membranes: applications in drug discovery and drug delivery, *Mol. Pharmaceutics* 6 (2009) 1264–1276.
- [10] R.M. Leblanc, Molecular recognition at Langmuir monolayers, *Curr. Opin. Chem. Biol.* 10 (2006) 529–536.

- [11] Y. Ebara, Y. Okahata, A kinetic study of concanavalin A binding to glycolipid monolayers by using a quartz crystal microbalance, *J. Am. Chem. Soc.* 116 (1994) 11209–11212.
- [12] S. Wang, R.M. Leblanc, Molecular recognition of concanavalin A on mannoside diacetylene lipid monolayer at the air–water interface, *Biochim. Biophys. Acta* 1419 (1999) 307–312.
- [13] R. Barbucci, A. Magnani, A. Chiumiento, D. Pasqui, I. Cangioli, S. Lamponi, Fibroblast cell behavior on bound and adsorbed fibronectin onto hyaluronan and sulfated hyaluronan substrates, *Biomacromolecules* 6 (2005) 638–645.
- [14] K.D. Hardman, C.F. Ainsworth, Structure of concanavalin A at 2.4- resolution, *Biochemistry* 11 (1972) 4910–4919.
- [15] J.W. Becker, G.N. Reeke Jr., B.A. Cunningham, G.M. Edelman, New evidence on the location of the saccharide-binding site of concanavalin A, *Nature* 259 (1976) 406–409.
- [16] M.I. Page, W.P. Jencks, Entropic contributions to rate accelerations in enzymic and intramolecular reactions and the chelate effect, *Proc. Natl. Acad. Sci. U. S. A.* 68 (1971) 1678–1683.
- [17] N. Horan, L. Yan, H. Isobe, G.W. Whitesides, D. Kahne, Nonstatistical binding of a protein to clustered carbohydrates, *Proc. Natl. Acad. Sci. U. S. A.* 96 (1999) 11782–11786.
- [18] B.T. Houseman, M. Mrksich, The role of ligand density in the enzymatic glycosylation of carbohydrates presented on self-assembled monolayers of alkanethiolates on gold, *Angew. Chem. Int. Ed.* 38 (1999) 782–785.
- [19] C.R. Yonzon, E. Jeoung, S. Zou, G.C. Schatz, M. Mrksich, R.P. Van Duyne, A comparative analysis of localized and propagating surface plasmon resonance sensors: the binding of concanavalin A to a monosaccharide functionalized self-assembled monolayer, *J. Am. Chem. Soc.* 126 (2004) 12669–12676.
- [20] Z. Shen, M. Huang, C. Xiao, Y. Zhang, X. Zeng, P. Wang, Nonlabeled quartz crystal microbalance biosensor for bacterial detection using carbohydrate and lectin recognitions, *Anal. Chem.* 79 (2007) 2312–2319.
- [21] C.F. Grant, V. Kanda, H. Yu, D.R. Bundle, M.T. McDermott, Optimization of immobilized bacterial disaccharides for surface plasmon resonance imaging measurements of antibody binding, *Langmuir* 24 (2008) 14125–14132.
- [22] A.L. Martin, B. Li, E.R. Gillies, Surface functionalization of nanomaterials with dendritic groups: toward enhanced binding to biological targets, *J. Am. Chem. Soc.* 131 (2009) 734–741.
- [23] J.E. Gestwicki, C.W. Cairo, L.E. Strong, K.A. Oetjen, L.L. Kiessling, Influencing receptor–ligand binding mechanisms with multivalent ligand architecture, *J. Am. Chem. Soc.* 124 (2002) 14922–14933.
- [24] D.A. Mann, M. Kanai, D.J. Maly, L.L. Kiessling, Probing low affinity and multivalent interactions with surface plasmon resonance: ligands for concanavalin A, *J. Am. Chem. Soc.* 120 (1998) 10575–10582.
- [25] J.D. Taylor, M.J. Linman, T. Wilkop, Q. Cheng, Regenerable tethered bilayer lipid membrane arrays for multiplexed label-free analysis of lipid–protein interactions on poly(dimethylsiloxane) microchips using SPR imaging, *Anal. Chem.* 81 (2009) 1146–1153.
- [26] H. Zheng, X. Du, Enhanced binding and biosensing of carbohydrate-functionalized monolayers to target proteins by surface molecular imprinting, *J. Phys. Chem. B* 113 (2009) 11330–11377.
- [27] H. Zheng, X. Du, Protein-directed spatial rearrangement of glycolipids at the air–water interface for bivalent protein binding: in situ infrared reflection absorption spectroscopy, *J. Phys. Chem. B* 114 (2010) 577–584.
- [28] C. Gege, J. Vogel, G. Bendas, U. Rothe, R.R. Schmidt, Synthesis of the sialyl Lewis X epitope attached to glycolipids with different core structures and their selectin-binding characteristics in a dynamic test system, *Chem. Eur. J.* 6 (2000) 111–122.
- [29] X. Du, Y. Wang, Directed assembly of binary monolayers with a high protein affinity: infrared reflection absorption spectroscopy (IRRAS) and surface plasmon resonance (SPR), *J. Phys. Chem. B* 111 (2007) 2347–2356.
- [30] T. Weimar, Recent trends in the application of evanescent wave biosensors, *Angew. Chem. Int. Ed.* 39 (2000) 1219–1221.
- [31] R.J. Whelan, T. Wohland, L. Neumann, B. Huang, B.K. Kobilka, R.N. Zare, Analysis of biomolecular interactions using a miniaturized surface plasmon resonance sensor, *Anal. Chem.* 74 (2002) 4570–4576.
- [32] X. Du, Y. Wang, Y. Ding, R. Guo, Protein-directed assembly of binary monolayers at the interface and surface patterns of protein on the monolayers, *Langmuir* 23 (2007) 8142–8149.
- [33] X. Du, V. Hlady, D. Britt, Langmuir monolayer approaches to protein recognition through molecular imprinting, *Biosens. Bioelectron.* 20 (2005) 2053–2060.
- [34] R.G. Snyder, H.L. Strauss, C.A. Elliger, Carbon–hydrogen stretching modes and the structure of n-alkyl chains. 1. Long, disordered chains, *J. Phys. Chem.* 86 (1982) 5145–5150.
- [35] D.G. Cameron, H.L. Casal, E.F. Gudgin, H.H. Mantsch, The gel phase of dipalmitoyl phosphatidylcholine. An infrared characterization of the acyl chain packing, *Biochim. Biophys. Acta* 596 (1980) 463–467.
- [36] Y. Wang, X. Du, Miscibility of binary monolayers at the air–water interface and interaction of protein with immobilized monolayers by surface plasmon resonance technique, *Langmuir* 22 (2006) 6195–6202.
- [37] R.F.A. Zwaal, R.A. Demel, B. Roelofsens, L.L.M. Deenen, The lipid bilayers concept of cell membranes, *Trends Biochem. Sci.* 1 (1976) 112–114.
- [38] C. Peetla, V. Labhasetwar, Biophysical characterization of nanoparticle–endothelial model cell membrane interactions, *Mol. Pharmaceutics* 5 (2008) 418–429.
- [39] S. Krimm, J. Bandekar, Vibrational spectroscopy and conformation of peptides, polypeptides, and proteins, *Adv. Protein Chem.* 38 (1986) 181–364.
- [40] D.M. Byler, H. Susi, Examination of the secondary structure of proteins by deconvoluted FTIR spectra, *Biopolymers* 25 (1986) 469–487.
- [41] F. Dousseau, M. Pezolet, Determination of the secondary structure content of proteins in aqueous solutions from their amide I and amide II infrared bands. Comparison between classical and partial least-squares methods, *Biochemistry* 29 (1990) 8771–8779.
- [42] N. Demirdoven, C.M. Cheatum, H.S. Chung, M. Khalil, J. Knoester, A. Tokmakoff, Two-dimensional infrared spectroscopy of antiparallel  $\beta$ -sheet secondary structure, *J. Am. Chem. Soc.* 126 (2004) 7981–7990.
- [43] H.S. Chung, A. Tokmakoff, Visualization and characterization of the infrared active amide I vibrations of proteins, *J. Phys. Chem. B* 110 (2006) 2888–2898.
- [44] Z. Derewenda, J. Yariv, J.R. Helliwell, A.J. Kalb, E.J. Dodson, M.Z. Papiz, T. Wan, J. Champbell, The structure of the saccharide-binding site of concanavalin A, *EMBO J.* 8 (1989) 2189–2193.
- [45] R. Mendelsohn, J.W. Brauner, A. Gericke, External infrared reflection absorption spectroscopy of monolayer films at the air–water interface, *Annu. Rev. Phys. Chem.* 46 (1995) 305–334.
- [46] C.R. Flach, A. Gericke, R. Mendelsohn, Quantitative determination of molecular chain tilt angles in monolayer films at the air/water interface–infrared reflection/absorption spectroscopy of behenic acid methyl ester, *J. Phys. Chem. B* 101 (1997) 58–65.
- [47] A. Gericke, C.R. Flach, R. Mendelsohn, Structure and orientation of lung surfactant SP-C and L- $\alpha$ -dipalmitoylphosphatidylcholine in aqueous monolayers, *Biophys. J.* 73 (1997) 492–499.
- [48] R. Mendelsohn, G. Mao, C.R. Flach, Infrared reflection–absorption spectroscopy: principles and applications to lipid–protein interaction in Langmuir films, *Biochim. Biophys. Acta* 1798 (2010) 788–800.
- [49] H. Yim, M.S. Kent, D.Y. Sasaki, B.D. Polizzotti, K.L. Kiick, J. Majewski, S. Satija, Rearrangement of lipid ordered phase upon protein adsorption due to multiple site binding, *Phys. Rev. Lett.* 96 (2006) 198101.
- [50] E. Stengberg, B. Persson, H. Roos, C. Urbaniczky, Quantitative determination of surface concentration of protein with surface plasmon resonance using radiolabeled proteins, *J. Colloid Interface Sci.* 143 (1991) 513–526.
- [51] D.E. Hansen, Recent developments in the molecular imprinting of proteins, *Biomaterials* 28 (2007) 4178–4191.
- [52] H. Dhruv, R. Pepalla, M. Taveras, D.W. Britt, Protein insertion and patterning of PEG bearing Langmuir monolayers, *Biotechnol. Progr.* 22 (2006) 150–155.